Eur. Phys. J. B **45**, 311–315 (2005)
DOI: 10.1140/epjb/e2005-00200-x

THE EUROPEAN PHYSICAL JOURNAL B

Strong Coulomb effects in hole-doped Heisenberg chains

J. Schnack[a]

Universität Osnabrück, Fachbereich Physik, 49069 Osnabrück, Germany

Received 9 February 2005 / Received in final form 7 April 2005
Published online 6 July 2005 –

Abstract. Substances such as the "telephone number compound" $Sr_{14}Cu_{24}O_{41}$ are intrinsically hole-doped. The involved interplay of spin and charge dynamics is a challenge for theory. In this article we propose to describe hole-doped Heisenberg spin rings by means of complete numerical diagonalization of a Heisenberg Hamiltonian that depends parametrically on hole positions and includes the screened Coulomb interaction among the holes. It is demonstrated that key observables like magnetic susceptibility, specific heat, and inelastic neutron scattering cross section depend sensitively on the dielectric constant of the screened Coulomb potential.

PACS. 75.10.Pq Spin chain models – 75.40.Mg Numerical simulation studies

1 Introduction and model

Substances hosting spin and charge degrees of freedom exhibit a large variety of phenomena like magnetic and charge ordering, metallic conductivity and superconductivity [1,2]. The "telephone number compound", $Sr_{14}Cu_{24}O_{41}$, contains two magnetic one-dimensional structures, chains and ladders. The stoichiometric formula suggests 6 holes per formula unit. We will assume that for the undoped compound all holes are located in the chain subsystem (i.e. 60% holes), although this is experimentally under discussion since X-ray absorption (XAS) measurements suggest that at room temperature some holes are located in the ladder subsystem [3], whereas it is necessary to assume that all holes are in the chain subsystem in order to explain neutron scattering data [4].

At low temperatures the ladder subsystem is magnetically inactive due to a large spin gap [5]. The remaining dynamics of the hole-doped chain system is still interesting as well as complicated enough to constitute a challenge for theoretical investigations. Especially the evaluation of thermodynamic quantities both as function of temperature and magnetic field is prohibitively complicated even for moderate system sizes. Therefore, mostly approximate descriptions in terms of classical spin dynamics [6,7], spin-dimer models [8–10] or spin-wave analysis [11] have been applied. Calculations based on the Hubbard model aim at ground-state correlations at low hole doping [12].

A fundamental question in this context is how the charge order in the CuO_2 chains of substances such as $Sr_{14}Cu_{24}O_{41}$ is established. These chains seem to be a sequence of rather perfect antiferromagnetically coupled spin dimers separated by holes, see Figure 1. Any proposed theoretical model should also be able to describe excitations involving hole motion which is crucial because interesting physical properties of these compounds result from a competition of charge mobility and magnetic interactions [13–16]. One possible explanation is that the formation of dimers is generated by structural modulations of the material via a strong variation of the on-site orbital energies [17–20].

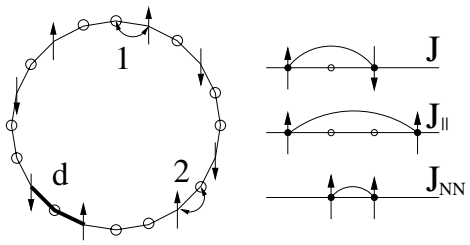

Fig. 1. L.h.s.: Ground-state hole configuration for 20 sites and 60% holes. This configuration is also called dimer configuration since it consists of weekly interacting antiferromagnetic dimers. One dimer is highlighted (d). The hole-spin exchange processes **1** and **2** lead to energetically low-lying configurations. R.h.s.: Exchange parameters used in this article: $J = -67$ K, $J_{\|} = 7$ K, and $J_{NN} = 25$ K.

In this article we investigate how a screened electrostatic hole-hole repulsion along the chain would express itself in thermodynamic quantities. It will turn out that a rather strong Coulomb repulsion is needed in order to reproduce the experimental magnetization. This is in accord with e.g. reference [21] or with references [22,23], where a dielectric constant of 3.3 is found to be realistic.

In order to be able to evaluate thermodynamic quantities we propose to describe hole-doped spin rings with

[a] e-mail: jschnack@uos.de

a Heisenberg Hamiltonian that depends parametrically on hole positions. This ansatz is similar to a simple Born-Oppenheimer description where the electronic Hamiltonian (here spin Hamiltonian) depends parametrically on the positions of the classical nuclei (here hole positions). Each configuration $\boldsymbol{c}$ of holes and spins defines a Hilbert space which is orthogonal to all Hilbert spaces arising from different configurations. The Hamilton operator $\underset{\sim}{H}(\boldsymbol{c})$ of a certain configuration $\boldsymbol{c}$ is of Heisenberg type and depends parametrically on the actual configuration $\boldsymbol{c}$, i.e.

$$\underset{\sim}{H} = \sum_{\boldsymbol{c}} \left(\underset{\sim}{H}(\boldsymbol{c}) + V(\boldsymbol{c}) \right) \tag{1}$$

$$\underset{\sim}{H}(\boldsymbol{c}) = -\sum_{u,v} J_{uv}(\boldsymbol{c})\ \underset{\sim}{\boldsymbol{s}}(u) \cdot \underset{\sim}{\boldsymbol{s}}(v). \tag{2}$$

$J_{uv}(\boldsymbol{c})$ are the respective exchange parameters which depend on the configuration of holes. $J < 0$ describes antiferromagnetic coupling, $J > 0$ ferromagnetic coupling.

Figure 1 shows on the l.h.s. as an example the ground-state hole configuration of $Sr_{14}Cu_{24}O_{41}$ [4,11,9] which is a sequence of spin-hole-spin dimers separated by two holes. Energetically excited configurations arise if holes are moved to other sites as depicted exemplarily by the exchange processes **1** and **2**. The r.h.s. of Figure 1 illustrates how the exchange parameters depend on the actual hole configuration. In this work three different exchange parameters are employed.

A key ingredient of the proposed model is the inclusion of the electrostatic interaction between holes which is modeled by a screened Coulomb potential

$$V(\boldsymbol{c}) = \frac{e^2}{4\pi\epsilon_0\,\epsilon_r\,r_0}\frac{1}{2}\sum_{u\neq v}\frac{1}{|u-v|}, \tag{3}$$

where $r_0 = 2.75$ Å is the distance between nearest neighbor sites on the ring. The dielectric constant ϵ_r is considered as the only free parameter in the present investigation. Several attempts have been undertaken to estimate the dielectric constant which yielded values for ϵ_r up to 30 [24–26]. In related projects where the exchange interaction of chain systems in cuprates is derived from hopping matrix elements between different orbitals using a Madelung potential the dielectric constant is found to be $\epsilon_r = 3.3$ [22,23].

2 Discussion of the model

The aim of the proposed model is to evaluate the complete spectrum for reasonably large system sizes and thus to be able to investigate thermodynamic quantities both as function of temperature and field. The spectrum does not only consist of those levels belonging to the ground-state hole distribution, compare Figure 1, but also of all levels arising from all other hole configurations. For small systems all such configurations can be generated and the related spin Hamiltonians (2) can be diagonalized completely. For 8 spins and 12 holes for instance this amounts to 6310 distinct hole configurations and tiny Hilbert spaces of dimension 256. For 16 spins and 24 holes the total number of hole configurations is already too big to be considered completely. Therefore, only the ground-state configuration and low-lying excitations with their respective degeneracies are taken into account. This is sufficient since hole configurations which deviate considerably from the ground state configuration possess very high excitation energies.

Correlated electrons are usually modeled with the Hubbard model [12], therefore looking at equations (1) and (2) one might be tempted to ask: *Where is the kinetic energy of the holes?* The Hamiltonian of the Hubbard model [27–29],

$$\underset{\sim}{H} = -\sum_{\langle ij\rangle,\sigma} t_{ij}\left(\underset{\sim}{c}^{\dagger}_{i\sigma}\underset{\sim}{c}_{j\sigma} + \text{h.c.}\right) + U\sum_i \underset{\sim}{n}_{i\uparrow}\underset{\sim}{n}_{i\downarrow}, \tag{4}$$

transforms at large U and half filling into a Heisenberg Hamiltonian (2) with $J_{ij} = -4t_{ij}^2/U$. Therefore, if working close to half filling, it is legitimate to say that the kinetic energy is absorbed into the exchange coupling. Nevertheless, the remaining hole motion is treated classically, i.e. superpositions of hole states are not taken into account. For the actual compound which is far from superconductivity this assumption of well-localized holes seems to be appropriate.

What is properly taken into account is the screened Coulomb interaction between holes. But, if so: *Wouldn't it be sufficient to consider nearest-neighbor Coulomb repulsion only?* Although this is a common method we find that a simple nearest-neighbor repulsion results in unphysical ground states. It is experimentally verified by means of low-temperature susceptibility [10], neutron scattering [4,11] as well as thermal expansion measurements [9], that the highly symmetric dimer configuration, compare Figure 1, constitutes the ground state of $Sr_{14}Cu_{24}O_{41}$. Using only nearest-neighbor Coulomb repulsion yields an alternating sequence of spins and holes with the remaining 10% holes assembling as a big cluster irrespective how strong the repulsion is. The reason is that this strange configuration has the same number of nearest hole-hole neighbors as the dimer configuration. Even the inclusion of a next-nearest neighbor Coulomb repulsion does not improve the situation, the Coulomb interaction is still proportional to the number of sites and may be overcome by the antiferromagnetic binding J.

3 Results

At temperatures and energies below 200 K the behavior of the chain subsystem in $Sr_{14}Cu_{24}O_{41}$ is usually discussed in terms of weakly interacting dimers sometimes augmented by weak interchain interactions, see e.g. [8–11]. Such a picture, although rather successful, does not allow to discuss the influence of mobile holes on thermodynamic observables. It is clear that configurations like **1** and **2** in Figure 1 will contribute to thermal averages, but how?

Figure 2 shows the low-energy part of the spectrum of a chain of $N_{\text{tot}} = 40$ sites with $N_{\text{s}} = 16$ spins and

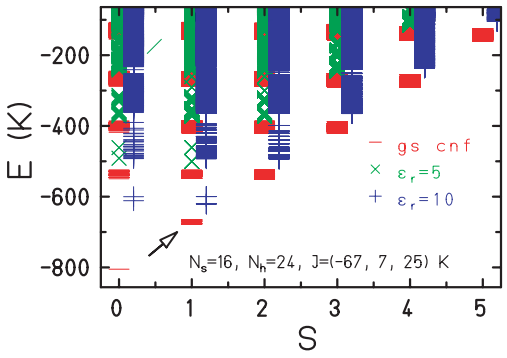

Fig. 2. Low-energy part of the spectrum of a chain of $N_{\rm tot} = 40$ sites with $N_{\rm s} = 16$ spins and $N_{\rm h} = 24$ holes for three choices of the dielectric constant ϵ_r: bars – $\epsilon_r = 1$, bars together with $\times$-symbols – $\epsilon_r = 5$, bars and crosses – $\epsilon_r = 10$. The arrow marks the singlet-triplet transition employed in dimer models.

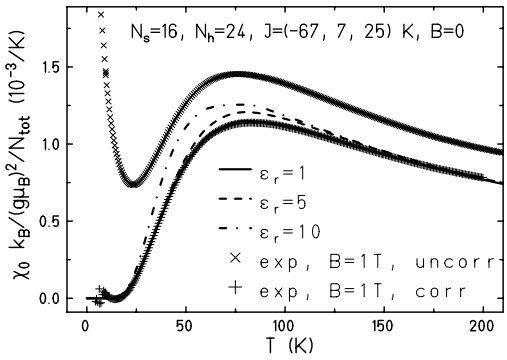

Fig. 3. Zero-field magnetic susceptibility $\chi_0(T)$: solid curve – $\epsilon_r = 1$, dashed curve – $\epsilon_r = 5$, dashed-dotted curve – $\epsilon_r = 10$. For a comparison experimental data, taken at $B = 1$ T, are provided by $\times$-symbols [10]. The corrected data, given by crosses, take also into account that due to impurities the number of dimers is less than theoretically possible [10].

$N_{\rm h} = 24$ holes for three choices of the dielectric constant ϵ_r. If $\epsilon_r = 1$ the spectrum up to several hundreds of Kelvin is solely given by the levels of the ground-state dimer configuration (bars in Fig. 2). With increasing ϵ_r the Coulomb repulsion decreases and so does the excitation energy of magnetic levels belonging to hole configurations where one or two holes are moved. As an example the levels resulting from such configurations are given as $\times$-symbols ($\epsilon_r = 5$) and crosses ($\epsilon_r = 10$) in Figure 2. It is clear that besides the singlet-triplet transition (arrow in Fig. 2), which is the main ingredient of the dimer model, transitions to states involving spin-holes exchange processes will contribute to thermodynamic observables like the inelastic neutron scattering cross section. In the following we discuss the influence on three basic observables.

Figure 3 presents the results for the magnetic susceptibility $\chi(T, B = 0) = \chi_0(T)$ at vanishing magnetic field $B = 0$. The solid curve shows the theoretical susceptibility for $\epsilon_r = 1$, the dashed curve for $\epsilon_r = 5$, and the dashed-dotted curve for $\epsilon_r = 10$. One realizes that with increasing

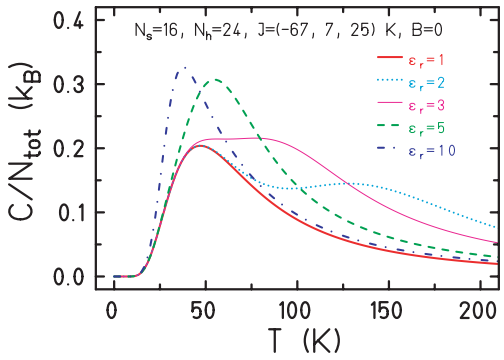

Fig. 4. Specific heat at $B = 0$: $\epsilon_r = 1$ – solid curve, $\epsilon_r = 2$ – dotted curve, $\epsilon_r = 3$ – thin curve, $\epsilon_r = 5$ – dashed curve, and $\epsilon_r = 10$ – dashed-dotted curve.

ϵ_r, i.e. with stronger screening of the Coulomb interaction, the susceptibility increases at intermediate temperatures and that the maximum shifts to lower temperatures. Although being rather moderate it is astonishing that the effect is at all observable since the responsible levels are at excitation energies well above that temperature range, compare the spectrum in Figure 2.

It turns out that the high degeneracy of excited hole configurations is the reason for the influence of the hole dynamics even at low temperatures. Looking again at the hole configuration shown in Figure 1 one notices that the spin-hole exchange processes can happen at very different places leading to a large geometric degeneracy. This degeneracy can overcompensate a small Boltzmann factor and thus expresses itself in a high thermal weight.

Together with the theoretical results Figure 3 shows the experimentally determined magnetization which was measured along the c-axis of the material at a magnetic field of $B = 1$ T [10]. The $\times$-symbols depict the uncorrected values whereas the crosses represent the corrected values. The correction includes a subtraction of impurities (free spins $s = 1/2$) as well as a rescaling because the number of dimers on the chain is less than theoretically possible. The almost perfect coincidence with the theoretical result for $\epsilon_r = 1$ suggests that the hole-hole repulsion is rather strong. The uncertainties in the measurement and the correction procedure leave some freedom for the actual value, but it is clear that ϵ_r should not be bigger than about three. This implies that energy levels which result from other than the dimer configuration are well above the triplet excitation, compare Figure 2. Although this might seem to be unrealistic one has to keep in mind that any theoretical model must explain why the experimental susceptibility practically coincides with that of free dimers. This is only possible if other excitations are well separated from the triplet excitation.

But even if higher-lying energy levels are well above the triplet excitation, due to their vast degeneracy they can substantially contribute to the specific heat, which is shown in Figure 4. In order to demonstrate how the thermal weight of the excited hole configurations grows several cases are shown. The solid curve, which is the lowest among all curves, again depicts the result for $\epsilon_r = 1$. With

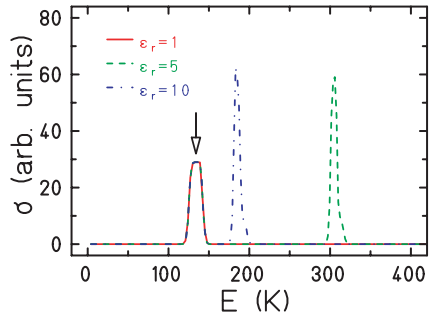

Fig. 5. Rough sketch of the lowest transitions observable with inelastic neutron scattering: $\epsilon_r = 1$ – solid curve, $\epsilon_r = 5$ – dashed curve, and $\epsilon_r = 10$ – dashed-dotted curve. The arrow marks the singlet-triplet transition at about 135 K.

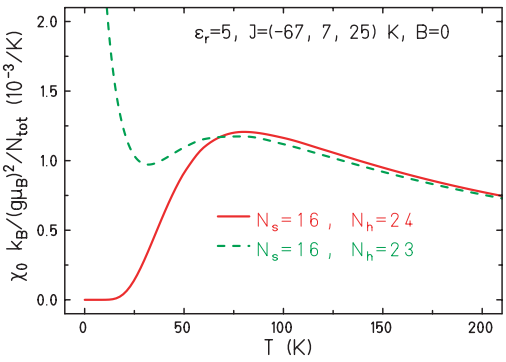

Fig. 6. Zero-field magnetic susceptibility $\chi_0(T)$ for $\epsilon_r = 5$: solid curve – $N_\mathrm{s} = 16$ and $N_\mathrm{h} = 24$, dashed curve – $N_\mathrm{s} = 16$ and $N_\mathrm{h} = 23$.

increasing dielectric constants thermal weight is shifted from higher temperatures to lower ones. This can very clearly be seen for the shown sequence: $\epsilon_r = 2$ (dotted curve), $\epsilon_r = 3$ (thin curve), $\epsilon_r = 5$ (dashed curve), and $\epsilon_r = 10$ (dashed-dotted curve). This result shows that for dielectric constants of the order of $\epsilon_r \approx 5$ about one third of the specific heat at its maximum is due to states involving hole motion.

Inelastic neutron scattering is a valuable tool to measure the magnetic excitation spectrum of substances like $Sr_{14}Cu_{24}O_{41}$, see e.g. [4,30]. The transition from the singlet ground state to the first excited triplet state, arrow in Figure 2, has been measured with high accuracy and used to determine the exchange constants, especially J (Fig. 1, r.h.s.). For recent results have a look at [30].

In addition to this fundamental transition of the dimer configuration, transitions to states with spin-hole exchange should be detectable, too. Figure 5 shows as a rough sketch where such transitions could be expected. The singlet-triplet transition at about 135 K – arrow in Figure 5 – is clearly seen for each dielectric constant. But with increasing ϵ_r transitions to states with one or two holes moved become accessible. The dashed curve shows schematically the lowest transitions for $\epsilon_r = 5$, the dashed-dotted curve the lowest transitions if $\epsilon_r = 10$. Although the singlet-triplet transition might have the largest matrix element, again the huge geometric degeneracy could help to make the other transitions visible. A possible drawback is, nevertheless, due to the fact that states involving spin-hole exchange break the translational symmetry, compare Figure 1. The momentum dependency, therefore, might be fuzzy.

4 Summary and outlook

For the compound under investigation the model is capable to address much more questions. Since it is not clear whether the hole content of the chain subsystem in $Sr_{14}Cu_{24}O_{41}$ is really 60%, one can study the influence of a reduced number of holes on magnetic observables.

Figure 6 shows as an example how a reduction by just one hole will influence the magnetic susceptibility. The perfect symmetry of successive spin-hole-spin dimers separated by two holes is destroyed and a low-lying triplet competes with the former singlet ground state which leads to a low-temperature divergence of the susceptibility. It might very well be that a part of the experimentally observed low-temperature divergence of the susceptibility [10] is due to the reduced hole doping of the chain.

The absence of perfect symmetry also leads to an increased mobility of the holes. At the imperfections neighboring holes can be moved without altering the Coulomb energy much. Therefore, the excitation energy for configurations where a hole is moved at imperfections will be rather low.

Summarizing, the main advantage of the proposed effective spin-hole Hamiltonian is that it allows to evaluate thermodynamic observables both as function of temperature and magnetic field for reasonably large systems. Using this model it could be shown how a hole-hole Coulomb repulsion along the chain would express itself in thermodynamic observables. The comparison with experimental magnetization data suggests that the screening is weak. The actual choice of the exchange parameters, compare Figure 1, does not influence the general conclusions about the effects of the Coulomb repulsion between holes. It is not yet clear whether a weekly screened Coulomb repulsion is realistic [21] or whether a combination of hole-hole Coulomb repulsion and modulation of on-site energies [17–20] has to be used. An experimental determination of other excited states than the triplet excitation of the dimers would be very helpful in this respect.

I would like to thank Bernd Büchner, Rüdiger Klingeler, Fatiha Ouchni, and Louis-Pierre Regnault for fruitful discussions, Rüdiger Klingeler for providing the experimental magnetization data, and Heinz-Jürgen Schmidt for carefully reading the manuscript.

References

1. E. Dagotto, Rev. Mod. Phys. **66**, 763 (1994)
2. V. Kataev et al., Phys. Rev. B **64**, 104422 (2001)
3. N. Nücker et al., Phys. Rev. B **62**, 14384 (2000)
4. L.P. Regnault et al., Phys. Rev. B **59**, 1055 (1999)

5. M. Takigawa, N. Motoyama, H. Eisaki, S. Uchida, Phys. Rev. B **57**, 1124 (1998)
6. M. Holtschneider, W. Selke, Phys. Rev. E **68**, 026120 (2003)
7. W. Selke, V.L. Pokrovsky, B. Büchner, T. Kroll, Eur. Phys. J. B **30**, 83 (2002)
8. S.A. Carter et al., Phys. Rev. Lett. **77**, 1378 (1996)
9. U. Ammerahl et al., Phys. Rev. B **62**, 8630 (2000)
10. R. Klingeler, *Spin- und Ladungsordnung in Übergangsmetalloxiden: Thermodynamische und magnetische Untersuchungen*, *Forschungsberichte aus den Naturwissenschaften / Physik* (Mensch & Buch Verlag, Berlin, 2003)
11. M. Matsuda, T. Yosihama, K. Kakurai, G. Shirane, Phys. Rev. B **59**, 1060 (1999)
12. R. Arita, K. Kuroki, H. Aoki, M. Fabrizio, Phys. Rev. B **57**, 10324 (1998)
13. S.A. Kivelson, E. Fradkin, V.J. Emery, Nature (London) **393**, 550 (1998)
14. A. Moreo, S. Yunoki, E. Dagotto, Science **283**, 2034 (1999)
15. J. Zaanen, Science **286**, 251 (1999)
16. C. Hess et al., Phys. Rev. Lett. **93**, 027005 (2004)
17. M. Isobe, E. Takayama-Muromachi, J. Phys. Soc. Jpn **67**, 3119 (1998)
18. A. Gelle, M.B. Lepetit, Phys. Rev. Lett. **92**, 236402 (2004)
19. A. Gelle, M.B. Lepetit, Eur. Phys. J. B **43**, 29 (2005)
20. A. Gelle, M.B. Lepetit, unpublished, `cond-mat/0410203`
21. B. Valenzuela, S. Fratini, D. Baeriswyl, Phys. Rev. B **68**, 045112 (2003)
22. Y. Mizuno et al., Phys. Rev. B **57**, 5326 (1998)
23. Y. Mizuno, T. Tohyama, S. Maekawa, Phys. Rev. B **58**, R14713 (1998)
24. C.Y. Chen et al., Phys. Rev. Lett. **63**, 2307 (1989)
25. F. Barriquand, G.A. Sawatzky, Phys. Rev. B **50**, 16649 (1994)
26. V.J. Emery, S.A. Kivelson, O. Zachar, Phys. Rev. B **56**, 6120 (1997)
27. J. Hubbard, Proc. R. Soc. London Ser. A-Math. **276**, 238 (1963)
28. J. Hubbard, Proc. R. Soc. London Ser. A-Math. **277**, 237 (1964)
29. J. Hubbard, Proc. R. Soc. London Ser. A-Math. **281**, 401 (1964)
30. C. Boullier et al., Physica B **350**, 40 (2004)